Journal of the Optical Society of America B
OPTICAL PHYSICS

Manipulating giant cross-Kerr nonlinearity at multiple frequencies in an atomic gaseous medium

Le van Doai, Nguyen Le Thuy An, Dinh Xuan Khoa, Vu Ngọc Sau, and Nguyen Huy Bang*

Department of Physics, Vinh University, 182 Le Duan Street, Vinh City, Vietnam
**Corresponding author: bangnh@vinhuni.edu.vn*

Received 9 May 2019; revised 6 July 2019; accepted 27 August 2019; posted 27 August 2019 (Doc. ID 367079); published 25 September 2019

We proposed a model for manipulating giant cross-Kerr nonlinearity in an atomic gaseous medium consisting of six-level inverted-Y systems. The absorption, dispersion, and cross-Kerr nonlinear coefficients of the medium are derived as analytical functions of the parameters of probe, coupling, and signal fields. It is shown that the cross-Kerr nonlinearity is enhanced significantly in three transparent windows under electromagnetically induced transparency (EIT). Furthermore, the cross-Kerr nonlinearity can be manipulated between positive and negative values by controlling intensity and/or frequency of the coupling laser. Such controllable giant cross-Kerr nonlinearity with the analytical interpretation is convenient to find experimental parameters and is useful for studying applications of controllable multi-channel quantum phase gates.

https://doi.org/10.1364/JOSAB.36.002856

1. INTRODUCTION

Electromagnetically induced transparency (EIT) is a quantum interference effect that may lead to a complete cancellation in resonant absorption of a weak probe field propagating through a medium in the presence of a strong coupling field [1]. The EIT effect can lead to a significant enhancement of Kerr nonlinearity of the atomic medium [1–3]. There are two widely used Kerr nonlinear effects involving self-Kerr or self-phase modulation (SPM) and cross-Kerr or cross-phase modulation (XPM) [4].

In most applications using a Kerr nonlinear effect [4], a strong nonlinear response of optical materials is often needed to enhance conversion efficiency and reduce input light intensity. Up to date, there is a large number of theoretical contributions [5–8] and experimental demonstrations [9–14] of the control and the enhancement of Kerr nonlinearity in the EIT media. Specifically, Schmidt and Imamoglu first proposed an N-type four-level system to obtain giant cross-Kerr nonlinearity under EIT conditions [5]. This scheme was experimentally demonstrated in cold Rb atoms by Kang *et al.* [10]. Later, Joshi and Xiao found large cross-Kerr nonlinearity in a four-level inverted-Y system that can be used to realize polarization quantum phase gates [6]. Xiao *et al.* [9] first measured the enhanced self-Kerr nonlinear coefficient in a three-level Λ-type atomic system of hot Rb atoms. For three-level atomic configurations, however, Kerr nonlinearity is only enhanced in a narrow spectrum region because it only produces one EIT window.

To create multiple EIT windows, use multilevel atomic systems excited by several coupling laser fields [15,16]. That is, if the N-level system excited by $(N-1)$ coupling laser fields, it is possible to create $(N-2)$ EIT windows. In recent years, some research groups have therefore focused on multilevel atomic systems to simultaneously control the enhanced nonlinearity at multiple frequencies [17–23]. Recently, we developed a simpler model to create multiple EIT windows with only one coupling laser field by using closely spaced hyperfine levels in quantum system that was first demonstrated in a five-level ladder-type ^{85}Rb atom [24]. The analytical model is applied for a five-level atomic system of Rb atoms and we obtained three-EIT windows on the absorption profile [25,26]. The analytical model has been used to interpret the experimental observations with a good agreement [27]. Along with the appearance of three-EIT windows on absorption line, self-Kerr nonlinearity is also enhanced at three different frequency regions [28]. This result also led to the appearance of optical bistability at multiple frequencies with low threshold intensity [29]. More recently, this system was developed to manipulate the multifrequency light velocity in the presence of self-Kerr nonlinearity [30] and Doppler broadening [31].

In this paper, we propose a six-level inverted-Y atomic system to enhance and manipulate the cross-Kerr nonlinearity at multiple frequencies. The expressions for absorption, dispersion, and cross-Kerr nonlinear coefficients of a six-level inverted-Y

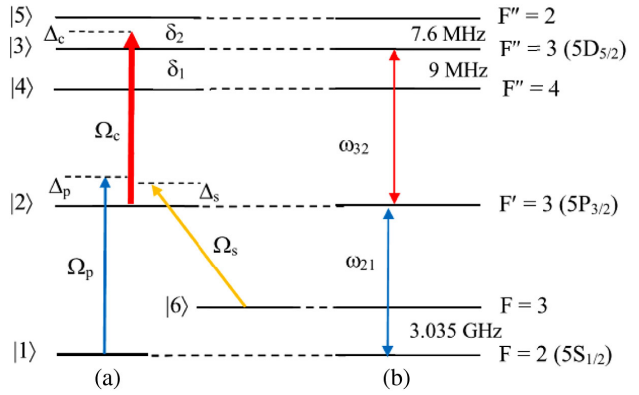

Fig. 1. (a) Six-level inverted-Y atomic system and (b) energy level diagram of ^{85}Rb atom.

atomic system were derived according to the parameters of laser fields. We show that the enhanced cross-Kerr nonlinearity with a reduced absorption can be simultaneously obtained at different frequencies. Moreover, the sign and magnitude of Kerr nonlinearity are investigated by adjusting the amplitudes and frequencies of the applied fields.

2. THEORETICAL MODEL

We consider a six-level inverted-Y atomic system interacting with three laser fields as depicted in Fig. 1(a). A weak probe laser field (with frequency ω_p and Rabi frequency Ω_p) drives the transition $|1\rangle \leftrightarrow |2\rangle$, whereas a strong coupling laser field (with frequency ω_c and Rabi frequency Ω_c) couples simultaneous transitions between state $|2\rangle$ and three closely spacing states–$|3\rangle$, $|4\rangle$, and $|5\rangle$. A signal laser field is applied to the transition, $|2\rangle \leftrightarrow |6\rangle$. The frequency separations between levels $|3\rangle-|4\rangle$ and $|5\rangle-|3\rangle$ are, respectively, denoted by δ_1 and δ_2. Experimentally, the scheme can be realized in the ^{85}Rb atom, with the states indicated in Fig. 1(b) [32], where the related states $|1\rangle$, $|2\rangle$, $|3\rangle$, $|4\rangle$, $|5\rangle$, and $|6\rangle$ are $5S_{1/2}(F=2)$, $5P_{3/2}(F''=3)$, $5D_{5/2}(F''=3)$, $5D_{5/2}(F''=4)$, $5D_{5/2}(F''=2)$, and $5S_{1/2}(F=3)$, respectively. The frequency separations between the closely spaced hyperfine levels are $\delta_1 = 9$ MHz and $\delta_2 = 7.6$ MHz.

The evolution of the system, which is represented via the density operator ρ, is represented by the Liouville equation,

$$\frac{\partial \rho}{\partial t} = -\frac{i}{\hbar}[H, \rho] + \Lambda\rho, \tag{1}$$

where H and $\Lambda\rho$ represent the total Hamiltonian and relaxation operator, respectively. Using the rotating-wave and the electric dipole approximations, the total Hamiltonian of the system in the interaction picture can be written as

$$H = \frac{\hbar}{2}\begin{pmatrix} 0 & \Omega_p & 0 & 0 & 0 & 0 \\ \Omega_p & 2(\Delta_p-\Delta_s) & \Omega_c a_{32} & \Omega_c a_{42} & \Omega_c a_{52} & \Omega_s \\ 0 & \Omega_c a_{32} & 2(\Delta_p+\Delta_c) & 0 & 0 & 0 \\ 0 & \Omega_c a_{42} & 0 & 2(\Delta_p+\Delta_c+\delta_1) & 0 & 0 \\ 0 & \Omega_c a_{52} & 0 & 0 & 2(\Delta_p+\Delta_c-\delta_2) & 0 \\ 0 & \Omega_s & 0 & 0 & 0 & 0 \end{pmatrix}, \tag{2}$$

where

$$\Delta_p = \omega_p - \omega_{21}, \quad \Delta_c = \omega_c - \omega_{32}, \quad \text{and} \quad \Delta_s = \omega_s - \omega_{62} \tag{3}$$

are frequency detuning of the probe, coupling, and signal lasers, respectively. From Eqs. (1) and (2) we derive the following equations of motion for the density matrix elements:

$$\dot{\rho}_{66} = -\Gamma_{62}\rho_{66} + \frac{i\Omega_s}{2}(\rho_{62} - \rho_{26}), \tag{4}$$

$$\dot{\rho}_{55} = -\Gamma_{52}\rho_{55} + \frac{i}{2}\Omega_c a_{52}(\rho_{52} - \rho_{25}), \tag{5}$$

$$\dot{\rho}_{44} = -\Gamma_{42}\rho_{44} + \frac{i}{2}\Omega_c a_{42}(\rho_{42} - \rho_{24}), \tag{6}$$

$$\dot{\rho}_{33} = -\Gamma_{32}\rho_{33} + \frac{i}{2}\Omega_c a_{32}(\rho_{32} - \rho_{23}), \tag{7}$$

$$\begin{aligned}\dot{\rho}_{22} = &-\Gamma_{21}\rho_{22} + \Gamma_{32}\rho_{33} + \Gamma_{42}\rho_{44} + \Gamma_{52}\rho_{55} + \Gamma_{62}\rho_{66} \\ &+ \frac{i}{2}\Omega_p(\rho_{21} - \rho_{12}) + \frac{i}{2}\Omega_c a_{32}(\rho_{23} - \rho_{32}) \\ &+ \frac{i}{2}\Omega_c a_{42}(\rho_{24} - \rho_{42}) + \frac{i}{2}\Omega_c a_{52}(\rho_{25} - \rho_{52}) \\ &+ \frac{i}{2}\Omega_s(\rho_{26} - \rho_{62}),\end{aligned} \tag{8}$$

$$\dot{\rho}_{11} = \Gamma_{21}\rho_{22} + \frac{i}{2}\Omega_p(\rho_{12} - \rho_{21}), \tag{9}$$

$$\begin{aligned}\dot{\rho}_{21} = &[i\Delta_p - \gamma_{21}]\rho_{21} + \frac{i}{2}\Omega_p(\rho_{22} - \rho_{11}) \\ &- \frac{i}{2}\Omega_c a_{32}\rho_{31} - \frac{i}{2}\Omega_c a_{42}\rho_{41} \\ &- \frac{i}{2}\Omega_c a_{52}\rho_{51} - \frac{i}{2}\Omega_s\rho_{61},\end{aligned} \tag{10}$$

$$\dot{\rho}_{31} = [i(\Delta_c + \Delta_p) - \gamma_{31}]\rho_{31} + \frac{i}{2}\Omega_p\rho_{32} - \frac{i}{2}\Omega_c a_{32}\rho_{21}, \tag{11}$$

$$\dot{\rho}_{41} = [i(\Delta_c + \Delta_p + \delta_1) - \gamma_{41}]\rho_{41} + \frac{i}{2}\Omega_p\rho_{42} - \frac{i}{2}\Omega_c a_{42}\rho_{21}, \tag{12}$$

$$\dot{\rho}_{51} = [i(\Delta_c + \Delta_p - \delta_2) - \gamma_{51}]\rho_{51} + \frac{i}{2}\Omega_p\rho_{52} - \frac{i}{2}\Omega_c a_{52}\rho_{21}, \tag{13}$$

$$\dot{\rho}_{61} = [i(\Delta_s - \Delta_p) - \gamma_{61}]\rho_{61} + \frac{i}{2}\Omega_p\rho_{62} - \frac{i}{2}\Omega_s\rho_{21}, \quad (14)$$

$$\dot{\rho}_{32} = [i\Delta_c - \gamma_{32}]\rho_{32} + \frac{i}{2}\Omega_p\rho_{31} + \frac{i}{2}\Omega_c a_{42}\rho_{34} + \frac{i}{2}\Omega_c a_{52}\rho_{35} + \frac{i}{2}\Omega_c a_{32}(\rho_{33} - \rho_{22}) + \frac{i}{2}\Omega_s\rho_{36}, \quad (15)$$

$$\dot{\rho}_{42} = [i(\Delta_c + \delta_1) - \gamma_{42}]\rho_{42} + \frac{i}{2}\Omega_p\rho_{41} + \frac{i}{2}\Omega_c a_{32}\rho_{43} + \frac{i}{2}\Omega_c a_{52}\rho_{45} + \frac{i}{2}\Omega_c a_{42}(\rho_{44} - \rho_{22}) + \frac{i}{2}\Omega_s\rho_{46}, \quad (16)$$

$$\dot{\rho}_{52} = [i(\Delta_c - \delta_2) - \gamma_{52}]\rho_{52} + \frac{i}{2}\Omega_p\rho_{51} + \frac{i}{2}\Omega_c a_{32}\rho_{53} + \frac{i}{2}\Omega_c a_{42}\rho_{54} + \frac{i}{2}\Omega_c a_{52}(\rho_{55} - \rho_{22}) + \frac{i}{2}\Omega_s\rho_{56}, \quad (17)$$

$$\dot{\rho}_{62} = [i\Delta_s - \gamma_{26}]\rho_{62} - \frac{i}{2}\Omega_s(\rho_{22} - \rho_{66}) + \frac{i}{2}\Omega_P\rho_{61} + \frac{i\Omega_c}{2}a_{32}\rho_{63} + \frac{i\Omega_c}{2}a_{42}\rho_{64} + \frac{i\Omega_c}{2}a_{52}\rho_{65}, \quad (18)$$

$$\dot{\rho}_{43} = [-i\delta_1 - \gamma_{43}]\rho_{43} + \frac{i}{2}\Omega_c a_{32}\rho_{42} - \frac{i}{2}\Omega_c a_{42}\rho_{23}, \quad (19)$$

$$\dot{\rho}_{53} = [-i\delta_2 - \gamma_{53}]\rho_{53} + \frac{i}{2}\Omega_c a_{32}\rho_{52} - \frac{i}{2}\Omega_c a_{52}\rho_{23}, \quad (20)$$

$$\dot{\rho}_{63} = [i(\Delta_s - \Delta_c) - \gamma_{36}]\rho_{63} + \frac{i}{2}\Omega_c a_{32}\rho_{62} - \frac{i}{2}\Omega_s\rho_{23}, \quad (21)$$

$$\dot{\rho}_{54} = [-i(\delta_1 + \delta_2) - \gamma_{54}]\rho_{54} + \frac{i}{2}\Omega_c a_{42}\rho_{52} - \frac{i}{2}\Omega_c a_{52}\rho_{24}, \quad (22)$$

$$\dot{\rho}_{64} = [i(\Delta_c - \Delta_s + \delta_1) - \gamma_{46}]\rho_{64} + \frac{i}{2}\Omega_c a_{42}\rho_{62} - \frac{i}{2}\Omega_s\rho_{24}, \quad (23)$$

$$\dot{\rho}_{65} = [-i(\Delta_c - \Delta_s - \delta_1) - \gamma_{56}]\rho_{65} + \frac{i}{2}\Omega_c a_{52}\rho_{62} - \frac{i}{2}\Omega_s\rho_{25}, \quad (24)$$

$$\rho_{ki} = \rho_{ik}^*, \quad (25)$$

$$\rho_{11} + \rho_{22} + \rho_{33} + \rho_{44} + \rho_{55} + \rho_{66} = 1, \quad (26)$$

where γ_{kl} is the coherence decay rate ρ_{kl}, which is determined as

$$\gamma_{kl} = \frac{1}{2}\left(\sum_{E_k<E_j}\Gamma_{jk} + \sum_{E_m<E_l}\Gamma_{lm}\right), \quad (27)$$

where Γ_{kl} is the population decay rate from level $|k\rangle$ to level $|l\rangle$; $\Omega_p = d_{21}E_p/\hbar$, $\Omega_c = d_{32}E_c/\hbar$, and $\Omega_s = d_{26}E_s/\hbar$ are Rabi frequency induced by the probe, coupling, and signal fields, respectively; d_{kl} is a dipole moment of the $|k\rangle - |l\rangle$ transition; $a_{32} = d_{32}/d_{32}$, $a_{42} = d_{42}/d_{32}$, and $a_{52} = d_{52}/d_{32}$ are the relative transition strengths. This means that the coupling intensity for the transitions $|2\rangle \leftrightarrow |3\rangle$, $|2\rangle \leftrightarrow |4\rangle$, and $|2\rangle \leftrightarrow |5\rangle$ are $\Omega_c a_{32}$, $\Omega_c a_{42}$, and $\Omega_c a_{52}$, respectively.

The density-matrix equations are solved under the steady-state condition to find the solutions for density matrix elements related to the probe and signal responses up to third order. Assuming that the coupling light intensity Ω_c is much stronger than the probe light intensity Ω_p and signal light intensity Ω_s, we obtain these equations from Eqs. (11)–(14):

$$\rho_{31} = \frac{i\Omega_c a_{32}}{2[i(\Delta_c + \Delta_p) - \gamma_{31}]}\rho_{21}, \quad (28)$$

$$\rho_{41} = \frac{i\Omega_c a_{42}}{2[i(\Delta_c + \Delta_p + \delta_1) - \gamma_{41}]}\rho_{21}, \quad (29)$$

$$\rho_{51} = \frac{i\Omega_c a_{52}}{2[i(\Delta_c + \Delta_p - \delta_2) - \gamma_{51}]}\rho_{21}, \quad (30)$$

$$\rho_{61} = \frac{i\Omega_s}{2[i(\Delta_p - \Delta_s) - \gamma_{61}]}\rho_{21} - \frac{i\Omega_p}{2[i(\Delta_p - \Delta_s) - \gamma_{61}]}\rho_{62}. \quad (31)$$

From Eq. (18) combined with Eqs. (21), (23), and (24), we find that

$$\rho_{62} = -\frac{i\Omega_s(\rho_{22} - \rho_{66})}{2(i\Delta_s + \gamma_{26}) + A} + \frac{i\Omega_P}{2(i\Delta_s + \gamma_{26}) + A}\rho_{61}, \quad (32)$$

where

$$A = \frac{\Omega_c^2 a_{32}^2}{2\,(i(\Delta_s + \Delta_c) + \gamma_{36})} + \frac{\Omega_c^2 a_{42}^2}{2\,(i(\Delta_s + \Delta_c + \delta_1) + \gamma_{46})} + \frac{\Omega_c^2 a_{52}^2}{2\,(i(\Delta_s + \Delta_c - \delta_2) + \gamma_{56})}. \quad (33)$$

By substituting Eq. (32) into Eq. (31) we have

$$\rho_{61} = \frac{i\Omega_s}{2\left(i(\Delta_p - \Delta_s) - \gamma_{61}\right)}\rho_{21} + \frac{\Omega_p\Omega_s(\rho_{66} - \rho_{22})}{2\,(2(i\Delta_s + \gamma_{26}) + A)\left(i(\Delta_p - \Delta_s) - \gamma_{61}\right)}. \quad (34)$$

By putting Eqs. (28)–(30) and (34) into Eq. (10) we find the solution for the density matrix element ρ_{21}, which relates to the first-order (in probe field Ω_p) and to the third-order (in signal field Ω_s) as

$$\rho_{21}=\frac{i\Omega_p(\rho_{11}-\rho_{22})}{2(i\Delta_p-\gamma_{21})+\frac{\Omega_s^2}{2\left(i(\Delta_p-\Delta_s)-\gamma_{61}\right)}+B}+\frac{i\Omega_p\Omega_s^2(\rho_{66}-\rho_{22})}{2\left(i(\Delta_p-\Delta_s)-\gamma_{61}\right)(2(i\Delta_s+\gamma_{26})+A)\left(2(i\Delta_p-\gamma_{21})+B\right)}, \tag{35}$$

where

$$B=\frac{\Omega_c^2a_{32}^2}{2\left(i(\Delta_c+\Delta_p)-\gamma_{31}\right)}+\frac{\Omega_c^2a_{42}^2}{2\left(i(\Delta_c+\Delta_p+\delta_1)-\gamma_{41}\right)}+\frac{\Omega_c^2a_{52}^2}{2\left(i(\Delta_c+\Delta_p-\delta_2)-\gamma_{51}\right)}. \tag{36}$$

Similarly, the solution for the density matrix element ρ_{26} that relates to the first-order (in signal field Ω_s) and to the third-order (in probe field Ω_p) is found as

$$\rho_{26}=\frac{i\Omega_s(\rho_{66}-\rho_{22})}{2(i\Delta_s-\gamma_{26})+\frac{\Omega_p^2}{2\left(i(\Delta_p-\Delta_s)+\gamma_{61}\right)}+N}+\frac{i\Omega_s\Omega_p^2(\rho_{11}-\rho_{22})}{2\left(i(\Delta_p-\Delta_s)+\gamma_{61}\right)\left(2(i\Delta_p+\gamma_{21})+M\right)(2(i\Delta_s-\gamma_{26})+N)}, \tag{37}$$

where

$$M=\frac{\Omega_c^2a_{32}^2}{2\left(i(\Delta_p+\Delta_c)+\gamma_{31}\right)}+\frac{\Omega_c^2a_{42}^2}{2\left(i(\Delta_p+\Delta_c+\delta_1)+\gamma_{41}\right)}+\frac{\Omega_c^2a_{52}^2}{2\left(i(\Delta_p+\Delta_c-\delta_2)+\gamma_{51}\right)}, \tag{38}$$

$$N=\frac{\Omega_c^2a_{32}^2}{2\left(i(\Delta_c+\Delta_s)-\gamma_{36}\right)}+\frac{\Omega_c^2a_{42}^2}{2\left(i(\Delta_c+\Delta_s+\delta_1)-\gamma_{46}\right)}+\frac{\Omega_c^2a_{52}^2}{2\left(i(\Delta_c+\Delta_s-\delta_2)-\gamma_{56}\right)}. \tag{39}$$

We note that the solutions ρ_{21} and ρ_{26} can be deduced in the case of the four-level atomic system as in [6], by setting $a_{42}=a_{52}=0$ in the expressions of A, B, M, and N.

The total susceptibilities can then be determined by

$$\chi_p=-2\frac{Nd_{21}}{\varepsilon_0E_p}\rho_{21}\equiv\chi_p^{(1)}+3E_s^2\chi_p^{(3)}, \tag{40}$$

$$\chi_s=-2\frac{Nd_{26}}{\varepsilon_0E_s}\rho_{26}\equiv\chi_s^{(1)}+3E_p^2\chi_s^{(3)}. \tag{41}$$

Therefore, the expressions for first- and third-order susceptibilities for the probe light field are determined by

$$\chi_p^{(1)}=-\frac{2Nd_{21}^2}{\hbar\varepsilon_0}\frac{i(\rho_{11}-\rho_{22})}{2(i\Delta_p-\gamma_{21})+\frac{\Omega_s^2}{2\left(i(\Delta_p-\Delta_s)-\gamma_{61}\right)}+B}, \tag{42}$$

$$\chi_p^{(3)}=-\frac{Nd_{21}^2d_{26}^2}{3\hbar^3\varepsilon_0}\times\frac{i(\rho_{66}-\rho_{22})}{\left(i(\Delta_p-\Delta_s)-\gamma_{61}\right)(2(i\Delta_s+\gamma_{26})+A)\left(2(i\Delta_p-\gamma_{21})+B\right)}. \tag{43}$$

Similarly, the expressions for first- and third-order susceptibilities for the signal light field is

$$\chi_s^{(1)}=-\frac{2Nd_{26}^2}{\hbar\varepsilon_0}\frac{i(\rho_{66}-\rho_{22})}{2(i\Delta_s-\gamma_{26})+\frac{\Omega_p^2}{2\left(i(\Delta_p-\Delta_s)+\gamma_{61}\right)}+N}, \tag{44}$$

$$\chi_s^{(3)}=-\frac{Nd_{21}^2d_{26}^2}{3\hbar^3\varepsilon_0}\times\frac{i(\rho_{11}-\rho_{22})}{\left(i(\Delta_p-\Delta_s)+\gamma_{61}\right)\left(2(i\Delta_p+\gamma_{21})+M\right)(2(i\Delta_s-\gamma_{26})+N)}. \tag{45}$$

From the first- and third-order susceptibilities, we find the linear dispersion n_0 and cross-Kerr nonlinear n_2 coefficients of six-level atomic system for the probe light is [4]

$$n_0=1+\frac{\mathrm{Re}(\chi_p^{(1)})}{2}, \tag{46}$$

$$n_2=\frac{3\mathrm{Re}\left(\chi_p^{(3)}\right)}{2\varepsilon_0n_0^2c}. \tag{47}$$

3. RESULTS AND DISCUSSION

To illustrate the analytical results, we apply cold ^{85}Rb atomic vapor as shown in Fig. 1(b), in which the atomic parameters are given by [24,32]: $N=10^{12}$ atoms/cm^3; $\Gamma_{32}=\Gamma_{42}=\Gamma_{52}=0.97$ MHz; $\Gamma_{21}=\Gamma_{62}=6$ MHz; $d_{21}=1.6\times10^{-29}$C.m; $\omega_p=3.77\times10^8$ MHz and $a_{32}:a_{42}:a_{52}=1:1.4:0.6$. For simplicity, all quantities related to frequency are given in units $\gamma=1$ MHz.

First of all, to see how cross-phase modulation changes at multiple frequencies, we plot probe susceptibility χ_p versus probe detuning Δ_p/γ and signal susceptibility χ_s versus signal detuning Δ_s/γ as shown in Fig. 2. In the presence of the strong coupling field, the EIT effect appears for both fields. In addition to the EIT window at the center of the absorption line $\Delta_p=0$ (or $\Delta_s=0$), there are two EIT windows that appear at

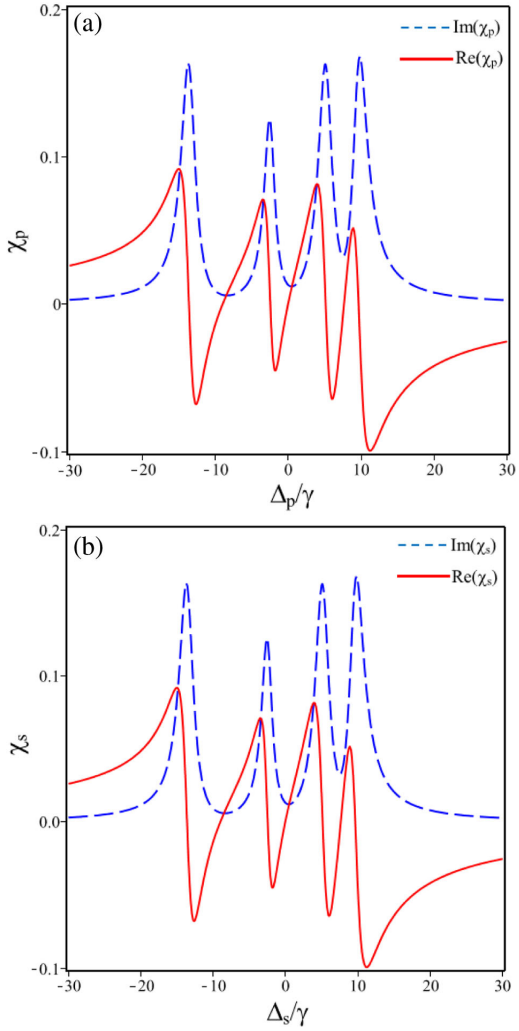

Fig. 2. (a) Change of probe susceptibility χ_p versus probe detuning Δ_p/γ when $\Delta_c = \Delta_s = 0$. (b) Variation of signal susceptibility χ_s versus signal detuning Δ_s/γ when $\Delta_c = \Delta_p = 0$. Other used parameters are $\Omega_p = \Omega_s = 0.1\gamma$ and $\Omega_c = 10\gamma$. The dashed and solid lines correspond to absorption and dispersion.

the positions $\Delta_p = -9\gamma$ and $\Delta_p = 7.6\gamma$ (or $\Delta_s = -9\gamma$ and $\Delta_s = 7.6\gamma$). Correspondingly, normal dispersion curves are also present in the three EIT windows, so the group velocity will be manipulated at three frequency regions. Under the resonance condition or equal detunings, the position of the EIT windows for the probe beam is identical to those for the signal beam. Therefore, the group velocity matching can also be realized, and cross-Kerr nonlinearity is also enhanced, as shown in Fig. 3.

In Fig. 3, we plot cross-Kerr nonlinearity n_2 (for the probe field) with the respect to probe detuning when $\Omega_p = \Omega_s = 0.1\gamma$, $\Omega_c = 6\gamma$, and $\Delta_c = \Delta_s = 0$. From the figure, it is clear that cross-Kerr nonlinearity is significantly enhanced around three transparent spectral regions at $\Delta_p = 0$, $\Delta_p = -9\gamma$, and $\Delta_p = 7.6\gamma$. Namely, in each transparent window, there is a pair of positive–negative peaks of n_2. In addition, the magnitude and sign of the cross-Kerr nonlinear coefficient can be controlled by adjusting the intensity and/or frequency of the coupling field as described in Figs. 4 and 5, respectively.

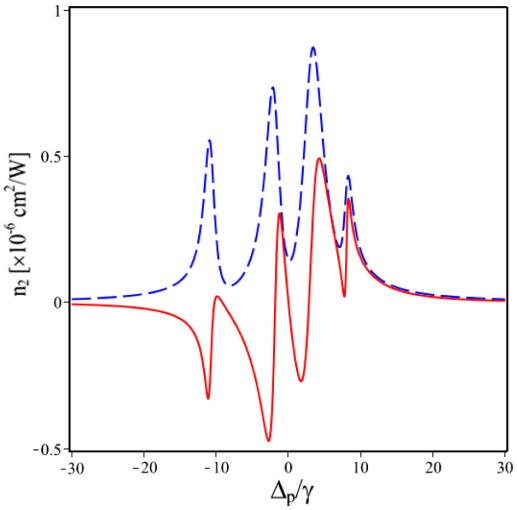

Fig. 3. Cross-Kerr nonlinear coefficient n_2 as a function of the probe detuning when $\Omega_p = \Omega_s = 0.1\gamma$, $\Omega_c = 6\gamma$ and $\Delta_c = \Delta_s = 0$. The dashed line represents absorption given by an imaginary part of Eq. (40).

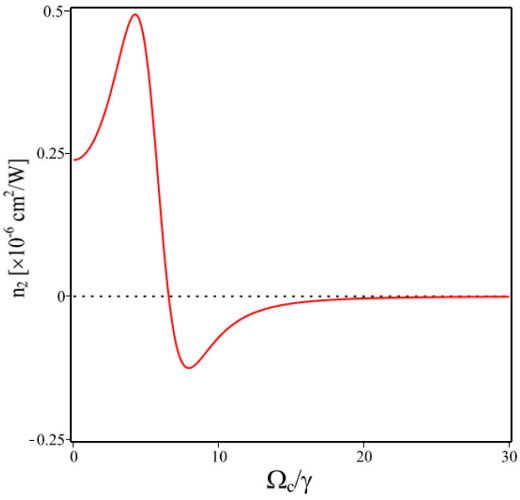

Fig. 4. Change of cross-Kerr nonlinearity according to coupling Rabi frequency Ω_c when $\Delta_p = 3\gamma$ and $\Delta_c = \Delta_s = 0$. The dotted line is zero.

In Fig. 4, we kept the detuning of the laser lights at $\Delta_p = 3\gamma$ and $\Delta_c = \Delta_s = 0$, which corresponds to a positive peak of n_2 in Fig. 3, and plotted the Kerr nonlinear coefficient versus Rabi frequency Ω_c. It is shown that we can switch between positive and negative values of n_2 by tuning the Rabi frequency of the coupling light by an amount of about $\Delta\Omega_c = 2.5\gamma$. Such variation comes from intensity dependence of the EIT efficiency, which results in an enhancement of Kerr nonlinearity [3,5]. In Fig. 5, we plotted the Kerr nonlinear coefficient versus frequency detuning Δ_c when other laser frequencies are kept at $\Delta_p = \Delta_s = 0$ and $\Omega_c = 3\gamma$. From Fig. 5 we also see that the Kerr nonlinear coefficient of the medium for the given frequency of probe laser has three pairs of positive–negative peaks of n_2 around $\Delta_c = 0$, $\Delta_c = -9\gamma$, and $\Delta_c = 7.6\gamma$.

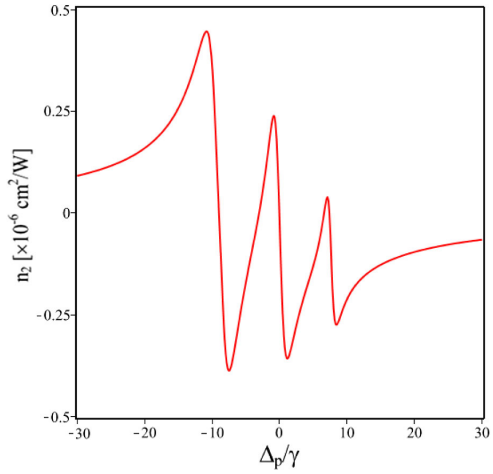

Fig. 5. Cross-Kerr nonlinear coefficient n_2 as a function of coupling frequency detuning Δ_c when $\Omega_c = 3\gamma$ and $\Delta_p = \Delta_s = 0$.

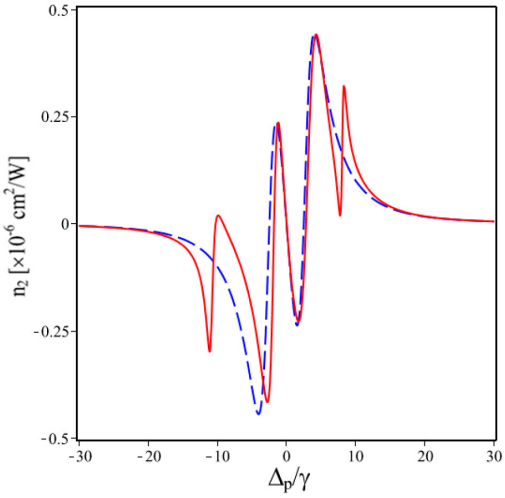

Fig. 6. Cross-Kerr nonlinear coefficient n_2 as a function of probe detuning in the case of the six-level (solid line) and four-level (dashed line) systems when $\Omega_p = \Omega_s = 0.1\gamma, \Omega_c = 6\gamma$ and $\Delta_c = \Delta_s = 0$.

Finally, in Fig. 6, we compared the behavior of cross-Kerr nonlinearity in the six-level and four-level systems, where levels $|4\rangle$ and $|5\rangle$ in the four-level system are neglected by setting $a_{42} = 0$ and $a_{52} = 0$ in expressions of A and B. It demonstrated that the cross-Kerr nonlinearity of the six-level system exhibits in a wider spectral region that corresponds to more positive and negative peaks of n_2. Namely, the six-level system has more possible ways to control the cross-Kerr nonlinearity that is needed for applications in multifrequency regions. For experimental realization of the six-level model, it could be arranged similarly to that in [10], except multifrequency probe light should be used. Here, the multifrequency probe light can be delivered from a single-mode laser with two appropriate acoustic modulators. As a consequence, the six-level inverted-Y system can be used for a multichannel quantum phase gate, in the same way that the single channel gate uses a four-level system in [6].

5. CONCLUSION

In this paper, we have proposed a model for the enhancement and manipulation of cross-Kerr nonlinearity at multiple frequencies in an atomic gaseous medium consisting of six-level inverted-Y systems. The expressions for absorption, dispersion, and cross-Kerr nonlinear coefficients of the medium are derived as a function of the parameters of probe, coupling, and signal fields. It is shown that in the presence of a strong coupling field the EIT effect with three-windows appears for both fields. The position of the EIT windows for the probe beam is identical to those for the signal beam. Therefore, the group velocity matching can also be realized and cross-Kerr nonlinearity is also enhanced greatly around three spectral regions corresponding to transparent windows. Moreover, the magnitude and sign of the cross-Kerr coefficient can be manipulated by tuning the frequency and/or the intensity of the coupling light. Such a controllable giant cross-Kerr nonlinearity with the analytical interpretation is convenient to find experimental parameters and is useful for studying applications of controllable multichannel quantum phase gates.

Funding. Vietnamese National Foundation of Science and Technology Development (NAFOSTED) (103.03-2017.332).

REFERENCES

1. S. E. Harris, "Electromagnetically induced transparency," Phys. Today **50**(7), 36 (1997).
2. M. Fleischhauer, A. Imamoglu, and J. P. Marangos, "Electromagnetically induced transparency: optics in coherent media," Rev. Mod. Phys. **77**, 633–673 (2005).
3. S. E. Harris, J. E. Field, and A. Imamoglu, "Non-linear optical processes using electromagnetically induced transparency," Phys. Rev. Lett. **64**, 1107 (1990).
4. R. W. Boyd, *Nonlinear Optics* (Academic, 1992).
5. H. Schmidt and A. Imamogdlu, "Giant Kerr nonlinearities obtained by electromagnetically induced transparency," Opt. Lett. **21**, 1936–1938 (1996).
6. A. Joshi and M. Xiao, "Phase gate with a four-level inverted-Y system," Phys. Rev. A **72**, 062319 (2005).
7. Y. P. Niu and S. Q. Gong, "Enhancing Kerr nonlinearity via spontaneously generated coherence," Phys. Rev. A **73**, 053811 (2006).
8. L. V. Doai, D. X. Khoa, and N. H. Bang, "EIT enhanced self-Kerr nonlinearity in the three-level lambda system under Doppler broadening," Phys. Scr. **90**, 045502 (2015).
9. H. Wang, D. Goorskey, and M. Xiao, "Enhanced Kerr nonlinearity via atomic coherence in a three-level atomic system," Phys. Rev. Lett. **87**, 073601 (2001).
10. H. Kang and Y. Zhu, "Observation of large Kerr nonlinearity at low light intensities," Phys. Rev. Lett. **91**, 093601 (2003).
11. H. Chang, Y. Du, J. Yao, C. Xie, and H. Wang, "Observation of cross-phase shift in hot atoms with quantum coherence," Europhys. Lett. **65**, 485–490 (2004).
12. J. Kou, R. G. Wan, Z. H. Kang, H. H. Wang, L. Jiang, X. J. Zhang, Y. Jiang, and J. Y. Gao, "EIT-assisted large cross-Kerr nonlinearity in a four-level inverted-Y atomic system," J. Opt. Soc. Am. B **27**, 2035–2039 (2010).
13. J. Sheng, X. Yang, H. Wu, and M. Xiao, "Modified self-Kerr-nonlinearity in a four-level N-type atomic system," Phys. Rev. A **84**, 053820 (2011).
14. X. D. Yang, S. J. Li, C. H. Zhang, and H. Wang, "Enhanced cross-Kerr nonlinearity via electromagnetically induced transparency in a four-level tripod atomic system," J. Opt. Soc. Am. B **26**, 1423–1434 (2009).

15. D. McGloin, D. J. Fullton, and M. H. Dunn, "Electromagnetically induced transparency in N-level cascade schemes," Opt. Commun. **190**, 221–229 (2001).
16. E. Paspalakis and P. L. Knight, "Electromagnetically induced transparency and controlled group velocity in a multilevel system," Phys. Rev. A **66**, 015802 (2002).
17. C. Ottaviani, S. Rebi, D. Vitali, and P. Tombesi, "Cross phase modulation in a five-level atomic medium: semiclassical theory," Eur. Phys. J. D **40**, 281–296 (2006).
18. Z.-B. Wang, K.-P. Marzlin, and B. C. Sanders, "Large cross- phase modulation between slow copropagating weak pulses in ^{87}Rb," Phys. Rev. Lett. **97**, 063901 (2006).
19. H. Sun, Y. Niu, S. Jin, and S. Gong, "Phase control of the Kerr nonlinearity in electromagnetically induced transparency media," J. Phys. B **41**, 065504 (2008).
20. M. Sahrai, S. H. Asadpour, and R. Sadighi, "Enhanced Kerr nonlinearity in a four-level EIT medium," J. Nonlinear Opt. Phys. Mater. **19**, 503–515 (2010).
21. X.-A. Yan, L.-Q. Wang, B.-Y. Yin, and J.-Q. Song, "Electromagnetically induced transparency and enhanced self-Kerr nonlinearity in a four-level scheme," Optik **122**, 986–990 (2011).
22. H. R. Hamedi and G. Juzeliunas, "Phase-sensitive Kerr nonlinearity for closed-loop quantum systems," Phys. Rev. A **91**, 053823 (2015).
23. H. R. Hamedi, A. H. Gharamaleki, and M. Sahrai, "Colossal Kerr nonlinearity based on electromagnetically induced transparency in a five-level double-ladder atomic system," Appl. Opt. **55**, 5892–5899 (2016).
24. J. Wang, L. B. Kong, X. H. Tu, K. J. Jiang, K. Li, H. W. Xiong, Y. Zhu, and M. S. Zhan, "Electromagnetically induced transparency in multi-level cascade scheme of cold rubidium atoms," Phys. Lett. A **328**, 437 (2004).
25. L. V. Doai, P. V. Trong, D. X. Khoa, and N. H. Bang, "Electromagnetically induced transparency in five-level cascade scheme of ^{85}Rb atoms: an analytical approach," Optik **125**, 3666–3669 (2014).
26. D. X. Khoa, P. V. Trong, L. V. Doai, and N. H. Bang, "Electromagnetically induced transparency in a five-level cascade system under Doppler broadening: an analytical approach," Phys. Scripta **91**, 035401 (2016).
27. D. X. Khoa, L. C. Trung, P. V. Thuan, L. V. Doai, and N. H. Bang, "Measurement of dispersive profile of a multi-window EIT spectrum in a Doppler-broadened atomic medium," J. Opt. Soc. Am. B **34**, 1255–1263 (2017).
28. D. X. Khoa, L. V. Doai, D. H. Son, and N. H. Bang, "Enhancement of self-Kerr nonlinearity via electromagnetically induced transparency in a five-level cascade system: an analytical approach," J. Opt. Soc. Am. B. **31**, 1330 (2014).
29. D. X. Khoa, L. V. Doai, L. N. M. Anh, L. C. Trung, P. V. Thuan, N. T. Dung, and N. H. Bang, "Optical bistability in a five-level cascade EIT medium: an analytical approach," J. Opt. Soc. Am. B **33**, 735–740 (2016).
30. N. T. Anh, L. V. Doai, and N. H. Bang, "Manipulating multi-frequency light in a five-level cascade-type atomic medium associated with giant self-Kerr nonlinearity," J. Opt. Soc. Am. B **35**, 1233–1239 (2018).
31. N. A. Tuan, L. V. Doai, D. H. Son, and N. H. Bang, "Manipulating multi-frequency light in a five-level cascade EIT medium under Doppler broadening," Optik **171**, 721–727 (2018).
32. D. A. Steck, "Rb^{85} D Line Data," http://steck.us/alkalidata.